losses, while that with Au the smallest, although these are of the same magnitude order of Ag and Al metals. **(Poster paper)**

1. M. N. Armenise, C. Canali, M. DeSario, A. Carnera, P. Mazzoldi, and G. Celotti, IEEE Trans. Components Hybrids Manuf. Technol. **CHMT-5,** 212 (June 1982).
2. M. N. Armenise, C. Canali, M. De Sario, A. Carnera, P. Mazzoldi, and G. Celotti, J. Appl. Phys. (Nov. 1982).
3. M. N. Armenise and M. De Sario, Fiber Integrated Opt. **3,** 197 (1980).
4. M. N. Armenise and M. De Sario, J. Opt. Soc. Am. **72,** 1514 (1982).
5. D. Marcuse and I. P. Kaminow, IEEE Trans. Quantum Electron. **QE-15,** 92 (1979).

TUM41 Paper withdrawn.

TUM42 Computer-controlled laser amplitude modulation

C.-C. HUANG, N. E. BUHOLZ, and J. SCHOLTZ, Lockheed Missiles & Space Co., P.O. Box 504, Sunnyvale, Calif. 94086.

Laser amplitude modulation having specific quadratic waveforms has been demonstrated. Reproduction of the desired waveforms is accomplished within 0.5%. The waveforms are computer generated and applied as discrete steps to a laser amplitude modulator. It is necessary to quiet the laser amplitude noise to within 0.1% and to compensate for the inherent nonlinearities of the modulation process. Although the functions here are quadratic, other waveforms, computer generated, would be applicable as well.

The method used to generate the quadratic waveforms is briefly described as follows. A set of numbers is derived by the microcomputer and transmitted to a digital-to-analog converter (DAC). The converter output voltage describes the ideal function and is applied via interface units to the acoustooptic laser amplitude modulator. A detected waveform of the resulting modulation (distorted by system nonlinearities) is returned to digital format via a DAC. The microcomputer then compares the ideal with received number sets. An adjustment is made in the transmitted set to bring the received set closer to the ideal function. This process is repeated until an acceptable accuracy is obtained, at which point the corresponding number set is continuously transmitted with no further modification.

Laser amplitude noise is quieted by taking a sample of the laser output before it reaches the quadratic function modulator and applying it with reverse phase into the modulation train. Near-perfect laser amplitude noise cancellation may be approached by using an optical fiber delay line to compensate the phase delay in the laser amplitude noise cancellation circuitry.

The system performance is shown in Fig. 1 with 0.5% peak-to-peak difference (middle trace) between the ideal wave forms (upper trace) and the detected waveforms (lower trace). **(Poster paper)**

TUM43 Instabilities in hybrid optical bistable devices with nonlinear feedback

J. A. MARTIN-PEREDA and M. A. MURIEL, Departamento de Electronica Cuantica ets. Ing. Telecommunicacion, U. P. M., Ciudad Universitaria, Madrid-3, Spain.

As we have shown,[1,2] several output conditions can be obtained from a hybrid optical bistable device when twisted nematic liquid crystal cells are employed as nonlinear elements. Depending on the amplification factor and/or the bias polarization, with a linear feedback, several different oscillations have been obtained having frequencies ranging from ~35 to 350 Hz. We extend these results to the case of a nonlinear feedback. Three different feedback devices have been employed. Both are represented in Fig. 1 where the black box corresponds, in the first case, to a classical electronic oscillator with different waveform and frequency outputs. In the second case, a Schmitt trigger works as the nonlinear feedback mechanism. In the third case, a hybrid electrooptical bistable device is added to the system.

The main difference between the first case and others is that the output frequency and waveform of the total system are imposed externally. When this external frequency matches the proper one of the fundamental hybrid optical bistable device *A* with linear feedback, several effects appear. If both frequencies are the same, the output signal corresponds to the one obtained in the linear case but with sharper shape. If the frequency ratio is a whole number, partial inhibition in the output signal occurs. If the ratio is not a whole number a mixture of signals appears.

The last two cases can be studied together because the second is an electronic simulation of the third.

The behavior is represented in Fig. 2. A clear hysteresis cycle appears in every case, where the real and simulated situations are indicated.

The second case, because it is based on an electronic Schmitt trigger, does not deserve further explanation.

In the last case, the nonlinear feedback is achieved by means of another twisted nematic liquid crystal cell configuration similar to the one employed in the basic branch (Fig. 1). This means that the cell forms a 45° angle with respect to the input laser beam and is placed between crossed polarizers. An electronic feedback, corresponding to a classical hybrid optical bistable system, is used. As we have studied, different situations appear depending on whether the ratio between amplification factors and bias voltages are the same in both systems; a situation close to tristability is obtained. But this situation is highly unstable giving rise to a random output signal. If amplification and bias are different in both systems, a quasi-chaotic output is achieved. This output is produced by a signal varying its frequency and amplitude with time. The mean frequency of this signal is ~180 Hz. The experiments were carried out with a stabilized 5-mW He–Ne laser. **(Poster paper)**

1. J. A. Martin-Pereda and M. A. Muriel, J. Opt. Soc. Am. **71,** 1640 (1981).
2. J. A. Martin-Pereda and M. A. Muriel, Appl. Phys. B **28,** 138 (1982).

TUM44 Diamond optoelectronic switch

P.-T. HO and CHI H. LEE, University of Maryland, Electrical Engineering Department, College Park, Md. 20742; J. C. STEPHENSON and R. R. CAVANAGH, U.S. National Bureau of Standards, Molecular Spectroscopy Division, Washington D.C. 20234.

We have succeeded in using natural diamond as a photoconductor to switch out high voltage by picosecond UV light pulses with 80% efficiency. Diamond is attractive in high-power applications for its excellent electrical insulation and thermal conduction.

The experimental arrangement is shown in Fig. 1. The diamond is 3 × 3 × 0.5 mm^3 in size. Electrical contact is made on the two large surfaces by silver paint spots of ~1.5-mm diam. The resistance between the contacts is over 20 MΩ, the limit of our capability. The diamond is inserted between the center leads of two coaxial cables, one of which has a 75-Ω characteristic impedance and is connected to a high-voltage source through a 160-kΩ resistor; the other is 50 Ω and terminated at the input of a Tektronix 7834 oscilloscope through a 200× attenuator. Ultraviolet light pulses of 1–1.5 mJ, frequency tripled from 30 psec, and 1.06-μm pulses from a Quantel 402 Nd:YAG laser, are focused on the diamond to a ~10-× 1.5-mm spot. With a bias voltage of 2.5 kV, the UV light is able to switch out ~800 V out of a possible maximum of 1000 V [2.5 kV × 50 Ω/(50 Ω + 75 Ω)], in a nanosecond which is associated with the bandwidth of the oscilloscope amplifier (model 7A19) (Fig. 2). Above 2.5 kV, discharge occurs near the electrodes. The switched-out voltage is fairly linear in both the bias voltage and in the UV light intensity, which seems to exclude charge carrier generation by two-photon valence-to-conduction band absorption. The second harmonic (5.3 μm) of the YAG laser produces similar results but requires ~10× the energy of the UV to switch out the same voltage from the same bias. The 1.06 μm does not switch out observable voltage. Data from another diamond sample of a different geometry are similar. Any further results will also be reported. **(Poster paper)**

TUM45 Performance evaluation of a high-speed high-resolution optical modulator

WALTER MOK, DAVID ARMITAGE, T. J. KARR, and F. JUNGA, Lockheed Palo Alto Research Laboratory, Electro-Optics Laboratory, 3251 Hanover St., Palo Alto, Calif. 94304.

Conventional light valves are typically low speed devices with limited resolution. They are tested and characterized in a continuous mode operation. The testing of our high-performance light valves required writing interference gratings into the light valve with a pulsed laser.

Experiments were conducted to measure the performance of a high-speed high-resolution solid-state optical light valve developed in Lockheed's Palo Alto Research Lab. The principle of operation was to record a pulsed interferogram on a fast response material and to simultaneously read it out with another strong readout beam. From the readout interferogram, we derive information about the linearity of the device as a function of bias voltage and input write light intensity, rise time, decay time constant, modulation transfer function, distortion, phase error, and signal-to-noise level.

The layout for the experiment is shown in Fig. 1. A doubled Nd:YAG laser (λ = 532 μm) is used to generate the interferogram on the input side of the light valve. The light valve is read out with an Ar^+ laser. The input and output spatial frequency and modulation are recorded on a high-resolution CCD array. The Ar^+ laser is operated in both cw and pulse mode. The MTF of the light valve was studied as a function of the time delay between the write and read beam. The rise time was measured with a high-speed photodiode located at the Fourier transform plane of the readout interferogram.

A programmable digital control circuit was built to time-sequence automatically all the operations of writing a pulse interferogram. The circuit commands the switching voltages applied to the light valve during its write/read cycles, fires the Nd:YAG laser, opens/closes shutters as required, and triggers the oscilloscope to display the detector signal. The circuit runs in write/read and erase modes and is capable of repetitive operation.

(Poster paper)

TUM40 Table I. Lossless Equivalent Indices n and R Ratio vs the Polar Angle for the Ordinary Guided Wave in a Multilayer Slab Waveguide with a Buffer Layer Having $n_b = 2.1$ and $t_d = 0.4$ μm; $\epsilon_{Au} = -10.22 - j0.96$, $t_{Au} = 200$ Å; Surface Change in Ordinary and Extraordinary Refractive Indices of $LiNbO_3$: $\Delta n_o = \Delta n_e = 0.04$ with Diffusion Length $d = 2$ μm and an erfc(x/d) Index Profile, $\lambda_0 = 0.6328$ μm, $LiNbO_3$ Substrate Indices $n_{os} = 2.286$ and $n_{es} = 2.200$

ϑ^0	R	Type	n	R	Type	n	R	Type	n
0	0.00	TE_0	2.303722	0.00	TE_1	2.290361	—	—	—
10	0.21	Q-TE_0	2.304052	0.24	Q-TE_1	2.290729	—	—	—
20	0.57	M-O	2.305278	0.58	M-1	2.292205	0.58	M-2	2.286343
30	0.82	M-O	2.308106	0.81	M-1	2.294782	0.81	M-2	2.287161
40	1.34	M-O	2.312861	1.10	M-1	2.296825	1.20	M-2	0.287628
50	2.04	M-O	2.318497	1.25	M-1	2.297897	1.67	M-2	2.287841
60	3.02	Q-TM_0	2.323766	2.10	Q-TM_1	2.298431	2.10	Q-TM_2	2.287947
70	4.83	SPW	2.327918	2.78	Q-TM_1	2.298702	2.82	Q-TM_2	2.288001
80	9.99	SPW	2.330546	5.72	Q-TM_1	2.298833	5.83	Q-TM_2	2.288027
90	∞	SPW	2.331443	∞	TM_1	2.298872	∞	TM_2	2.288035

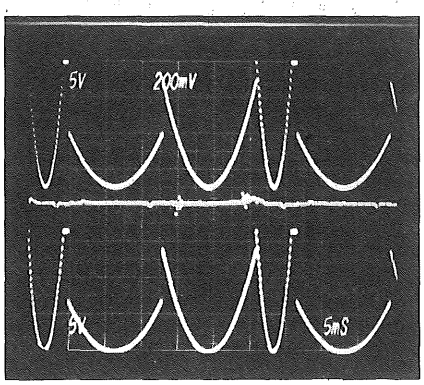

TUM42 Fig. 1. Computer-controlled laser amplitude modulation.

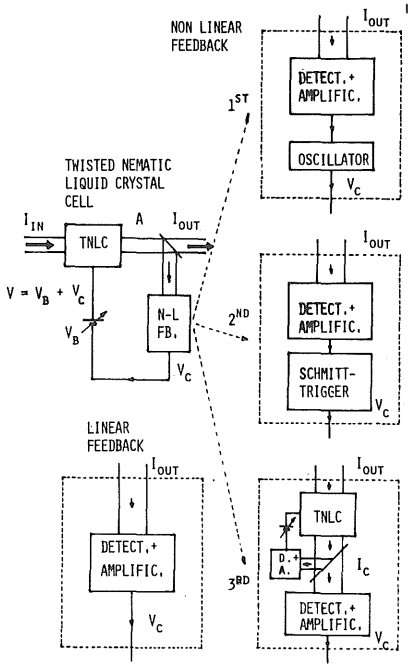

TUM43 Fig. 1. Feedback devices.

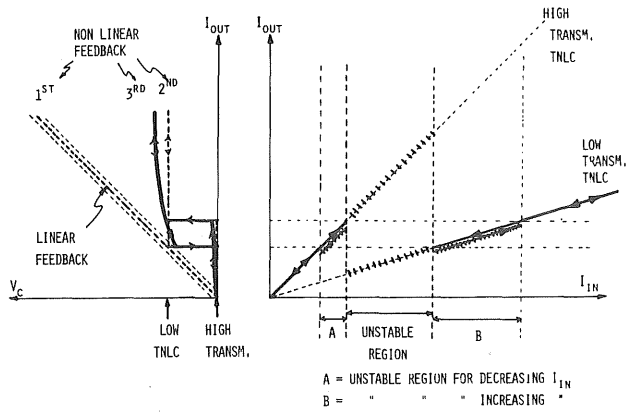

TUM43 Fig. 2. Output for various feedback devices as a function of input.

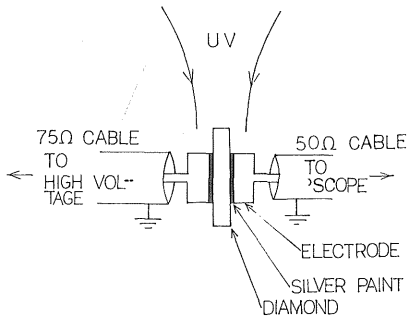

TUM44 Fig. 1. Diamond switch.

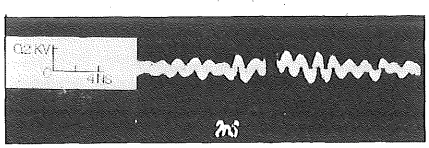

TUM44 Fig. 2. Switched-out voltage.

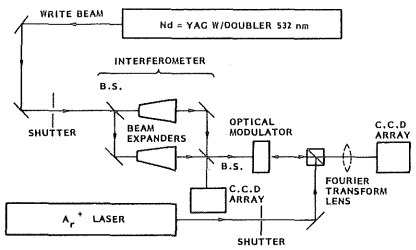

TUM45 Fig. 1. Layout for the optical light modulator evaluation experiment.